9390 *Macromolecules* **2009**, *42*, 9390–9393
DOI: 10.1021/ma901955c

Macromolecules
COMMUNICATION TO THE EDITOR

Controlling Poly(3-hexylthiophene) Crystal Dimension: Nanowhiskers and Nanoribbons

Jianhua Liu,[†] Mohammad Arif,[‡] Jianhua Zou,[†] Saiful I. Khondaker,[‡] and Lei Zhai*,[†]

[†]*NanoScience Technology Center and Department of Chemistry,* [‡]*NanoScience Technology Center and Department of Physics, and University of Central Florida, 12424 Research Parkway Suite 400, Orlando, Florida 32826*

Received September 2, 2009
Revised Manuscript Received November 2, 2009

Regioregular poly(3-hexylthiophene) (P3HT) is a promising semiconductive material for low-cost, large-scale, and flexible electronics such as thin film solar cells and field-effect transistors.[1−3] In these devices, P3HT is usually deposited from its solutions and then crystallizes dynamically into polycrystalline thin films upon solidification. The crystalline structure and morphology of P3HT significantly affect the thin film charge transport properties and consequently dominate the device performance. Understanding P3HT crystallization and controlling the crystal dimension is important to improve device performance as well as to design new semiconductive polymers with high charge mobility.[4−6] Extensive work on the crystallization of P3HT reveals a very complex process influenced by many factors such as thermal treatments,[7,8] solvents,[9,10] film thickness,[11] and polymer molecular weight (M_n).[12−14] In searching a theory to guide the study of complicated P3HT crystallization, we found that P3HT shares similar crystallization behavior with polyethylene (PE, a semicrystalline polymer) despite their different crystal morphology. The crystallization of traditional semicrystalline polymers such as PE has been well elucidated through the investigations of polymer solution crystals.[15] It is found that (1) polymer usually crystallizes into thin and lamellar single crystals in dilute solutions, (2) polymer chain folding occurs in the lamellar crystals, (3) the lamellar thickness (i.e., fold length) varies with crystallization temperature, and (4) lamellar crystals formed in dilute solutions are fundamental structures in complex crystals formed at high concentration and melt. In comparison to PE's crystallization behavior, P3HT forms one-dimensional (1D) lamellar crystals (nanowhiskers) from its dilute solutions via the $\pi-\pi$ interactions among polymer backbones,[16−19] while PE forms two-dimensional (2D) lamellar crystals. Typically, P3HT nanowhiskers have an average width of 13−15 nm and the thickness of 3−5 nm corresponding to two or three P3HT monolayers.[20] On the basis of the observation of smaller nanowhisker width compared to the polymer contour length,[21−23] polymer chain folding, a common phenomenon in PE crystallization, was proposed in P3HT nanowhiskers. Polycrystalline film of P3HT deposited at high concentration is composed of 1D nanowhisker-like domains comparable to the crystals formed in dilute solutions.[24] These observations suggest that a systematic investigation of P3HT crystals in solutions with the guidance of traditional crystallization theory will lead to further understanding of P3HT crystallization process and offer an opportunity to control the crystal dimension. Here we present a systematic investigation of P3HT crystallization by changing the polymer molecular weight (M_n), crystallization temperature, and polymer concentration. P3HT polymer chains change from extending to folding in nanowhiskers when the M_n is above a critical value, and the fold length can be controlled by changing the crystallization temperature. Such observation provides the first experimental support of P3HT chain folding when P3HT crystallizes from solutions. Furthermore, 1D nanowhiskers composed of extended P3HT chains can grow into highly ordered two-dimensional (2D) nanoribbons from more concentrated P3HT solutions, generating a new class of large P3HT crystals.

*Corresponding author. E-mail: lzhai@mail.ucf.edu.

Table 1. P3HT with Different Molecular Weight Used To Prepare Nanowhiskers in Solutions

sample	M_n[a] (kDa)	PDI[a]	corrected M_n[b] (kDa)	contour length[c] (nm)	average nanowhisker width[d] (nm)
A	6.0	1.50	3.6	8.4	7.3 ± 0.74
B	10.2	1.22	6.1	14.3	13.3 ± 0.63
C	15.6	1.25	9.3	21.9	14.6 ± 0.42
D	33.5	1.48	19.9	49.2	14.4 ± 0.35

[a] Number-average molecular weight (M_n) and polydispersity index (PDI) determined by GPC as shown in Figure S1. [b] Calculated from M_n determined by GPC by assuming that it overestimates the molecular weight by 70% (scaling factor: 1.7).[19] [c] Calculated according to the corrected M_n. [d] Average width determined by TEM, margin of error indicating a 95% confidence interval of the average width.

In order to systematically investigate the influence of P3HT molecular weight on the dimension of their crystalline structures (1D nanowhiskers), P3HTs with different M_n (sample A to sample D in Table 1) were first dissolved in their marginal solvents[25] at 90 °C and cooled down to room temperature (25 °C). P3HT precipitated out and formed 1D nanowhisker dispersion because of its low solubility in the marginal solvent at room temperature. Figure 1A−D shows the TEM images of the obtained nanowhiskers corresponding to sample A to sample D, respectively. A typical selected area electron diffraction (SAED) pattern is given in the inset of Figure 1D, which confirms the well-defined 1D structure in nanowhiskers.[17,21] The average widths of the nanowhiskers determined by TEM are listed in Table 1. Comparing to the contour lengths calculated from their corrected M_n (Table 1), the average nanowhisker widths of sample A and sample B are approximate to their corresponding contour lengths, while the average nanowhisker widths of sample C and D are constant regardless of their molecular weight and are much smaller than their corresponding contour lengths. The results suggest that P3HT polymer backbones in nanowhiskers will change from fully extending to folding at a critical M_n range. Traditional flexible semicrystalline polymers also show this M_n determined chain folding in their crystallization processes.[26,27] The critical M_n for P3HT chain folding is found to be around 10 kDa (determined by GPC) by comparing the nanowhisker widths of samples A−D. The nanowhisker width equals to the length of extended polymer chain and is proportional to M_n (samples A, B) when M_n is less than 10 kDa. In contrast, the width of nanowhiskers is constant regardless of M_n when M_n is above 10 kDa. Figure 1E shows the cartoons of nanowhiskers formed from P3HT with extended and folded polymer chains. Although P3HT is a rodlike polymer comparing with flexible polymers, it can form U-turn type fold, where several thiophene rings adopt a continuous *cis* conformation promoted by intramolecular alkyl side chain interactions.[28,29]

According to the traditional crystallization theory, the fold length is proportional to $1/\Delta T$ ($\Delta T = T_s^\circ - T_c$, where T_c and T_s°

 Published on Web 11/16/2009

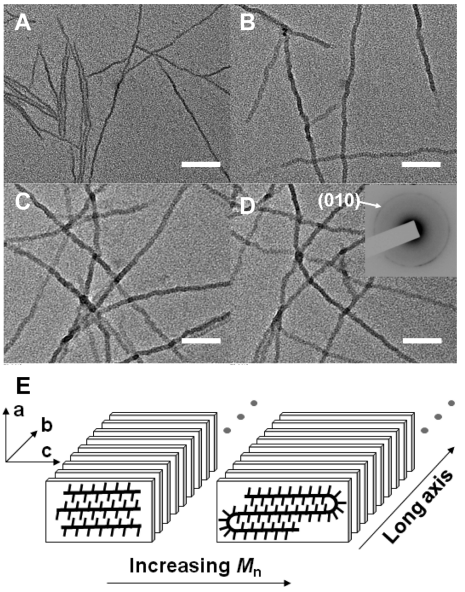

Figure 1. (A−D) TEM images of P3HT nanowhiskers prepared by a solution method at 25 °C, corresponding to samples A−D, respectively. Concentration: 0.20 mg/mL in DMF/anisole (volume ratio: 2:1) for sample A; 0.05 mg/mL in anisole for B, C, and D. Scale bar: 100 nm. Inset in (D): selected area electron diffraction pattern of P3HT nanowhisker of sample D. (E) Schematic illustration of extended (left) and folded (right) P3HT backbone stacking in nanowhiskers prepared by low M_n (left) and high M_n (right) P3HT, respectively. The U-turn of the polymer includes 6−7 alkylthiophene rings.

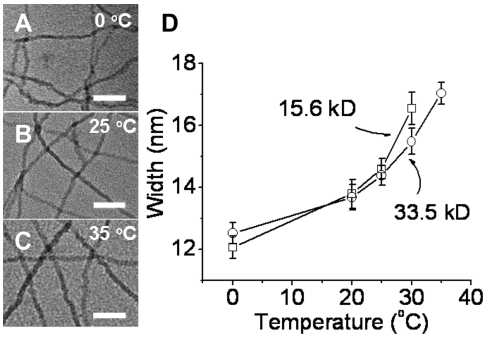

Figure 2. (A−C) TEM images of P3HT (33.5 kDa) nanowhiskers prepared at 0, 25, and 35 °C, respectively. Scale bar: 100 nm. (D) Curves for TEM determined average width of P3HT (square: 15.6 kDa; circle: 33.5 kDa) nanowhiskers versus crystallization temperatures.

are crystallization temperature and the dissolution temperature, respectively).[7] Higher T_c always leads to longer fold length in lamellar crystals. Therefore, the nanowhisker width can be increased by raising crystallization temperature if P3HT follows the traditional crystallization theory. To examine the hypothesis, crystals (nanowhiskers) of sample C and sample D were generated at different crystallization temperatures. The width of obtained nanowhiskers was examined by TEM. Figures 2A−C are the TEM images of nanowhiskers (sample D, 33.5 kDa) obtained at different temperature. As observed in the TEM images, the nanowhisker width increases with the increment of crystallization temperature. Figure 2D gives the plots of average nanowhisker width versus crystallization temperature of samples C and D. The average width of P3HT nanowhisker (sample D) varies from about 12.0 to 17.0 nm when crystallization temperature is increased from 0 to 35 °C. Comparing with sample D, sample C shows a larger increasing rate of nanowhisker width versus temperature, probably attributed to a lower dissolution temperature for lower molecular weight P3HT. Nevertheless, both polymers show a similar trend of increasing width with increasing temperature. Such observations not only confirm that the chain folding of rigid-rod P3HT is similar to that of semicrystalline flexible polymers, supporting the feasibility of considering the crystallization of P3HT according to semicrystalline flexible polymer crystallization theory, but also offer a simple approach to control the crystal dimension.

In the traditional crystallization theory, the morphology of polymer crystals formed at melt (spherulites) is more complex than polymer single crystals formed from a dilute solution although both have similar lamellar structures. Polymer crystals formed from a concentrated solution can be regarded as the intermediate of crystals obtained from a dilution solution and melt, and its morphology is more similar to that of the melt crystals.[30] P3HT polycrystalline films in organic electronics are usually fabricated by depositing its solutions on substrates followed by a thermal annealing. Therefore, P3HT polycrystalline film should have more comparable structure and morphology to P3HT crystals obtained from concentrated solutions than polymer single crystals obtained in dilute solutions.

For samples with fully extended chains (samples A and B), their crystal structures transform from 1D nanowhiskers to 2D nanoribbons or 2D nanoribbon aggregates with increased P3HT concentration (0.2−0.5 mg/mL). It is the first time that such P3HT 2D nanoribbon structures were obtained from P3HT solutions. Parts A and B of Figure 3 (more images in Figure S2) show the TEM images of P3HT nanoribbons obtained from sample A and B, respectively. The corresponding AFM images are shown in Figure 3C,D. Both the TEM and AFM images confirm the nanoribbon structures. 2D nanoribbons prepared from sample A are more uniform than those prepared from sample B. Its average length and width are about 1.0−1.5 μm and 250 nm, respectively. For sample B, small amount of nanowhiskers are observed beside irregular nanoribbons. The length of nanoribbons varies from 2 to 5 μm while the width varies from 50 to 200 nm, showing a higher aspect ratio than that of sample A. According to the cross-section analysis of AFM images, the P3HT nanoribbon thicknesses of samples A and B are 7.5 and 14.8 nm, respectively. Such measured thicknesses are very close to the contour lengths of corresponding P3HT (Table 1) as well as the widths of their nanowhiskers formed in dilute solutions. This observation suggests that the nanoribbon thickness corresponds to the length of a fully extended polymer chain. Figure 3E shows the SAED pattern of P3HT nanoribbons obtained from sample B. Different from the SAED pattern of 1D nanowhiskers (inset in Figure 1D), the SAED pattern of nanoribbons clearly shows both (010) reflection and (h00) reflections (h = 1, 2, 3), demonstrating 2D ordered characteristic of P3HT nanoribbons. Therefore, the molecular orientation in P3HT 2D nanoribbons should be stacked as shown in Figure 3F.

2D P3HT nanoribbons form through a further growth of 1D nanowhiskers as shown in Figure 3G. First, the $\pi-\pi$ interaction of P3HT generates 1D nanowhisker-like nucleus in solution; then the regioregular alkyl chains of extended P3HT on nanowhisker surface promote the growth along another direction [100] via alkyl interactions, leading to 2D nanoribbons. Since both the $\pi-\pi$ interaction and alkyl interaction influence the nanoribbon formation, they can be tuned to control the dimension of nanoribbons. Compared to sample A, sample B has a higher molecular weight with stronger intermolecular $\pi-\pi$ interactions, resulting in nanoribbons with a higher aspect ratio. In our studies, the yield of the nanoribbon formation was found to be more than 70% by comparing the solution UV−vis absorbance before and after the nanoribbon formation according to the reported approach.[20]

To examine the effect of large P3HT nanoribbon crystalline on charge transport property, we compared the charge mobility of

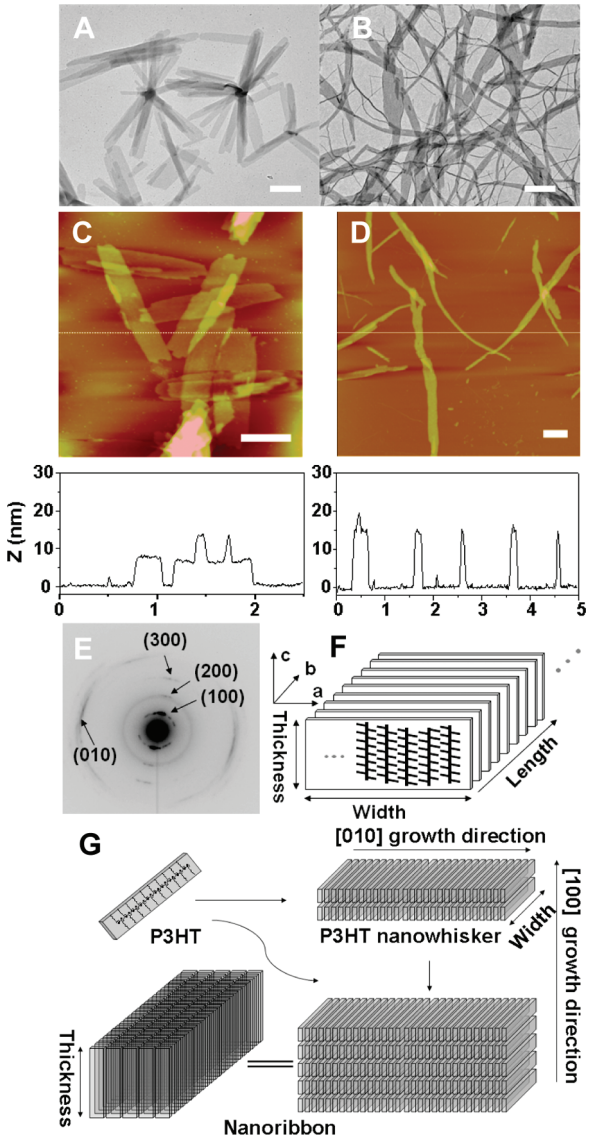

Figure 3. (A, B) TEM image of P3HT (6.0 and 10.2 kDa, respectively) nanoribbons. (C, D) Tapping-mode AFM height images (top) and their cross sections of the line trace (bottom) of P3HT nanoribbons (C: 6.0 kDa, 2.5 × 2.5 um; D: 10.2 kDa, 5.0 × 5.0 um) on silicon wafers (SiO_2/Si substrates) by spinning-coating. Scale bar: 500 nm. (E) Selected area electron diffraction pattern corresponding to P3HT (10.2 kDa) nanoribbon (B) with the electron beam perpendicular to the substrate. (F) Schematic illustration of molecular stacking in P3HT nanoribbon (G) Schematic illustration of the formation of P3HT nanoribbons.

P3HT films deposited from P3HT nanoribbon dispersion (sample B) and the solution of sample B in dichlorobenzene using a bottom gated field-effect transistor (FET). Since thermal annealing has been proved to be an effective approach to crystallize amorphous P3HT and improve the charge mobility of P3HT based devices,[31] both devices was annealed at 150 °C for 20 min to improve the order of the materials and electrode contact. The AFM image of the FET device after annealing (Figure S3) shows that the morphology of nanoribbon film was preserved. The characterization of FET devices shows that the device fabricated from the P3HT nanoribbon dispersion has a high charge mobility of 0.012 $cm^2/(V\ s)$ (on/off ratio: 6.5×10^4) (Figure 4), while the control device fabricated from a solution of sample B shows a mobility of 1.7×10^{-3} $cm^2/(V\ s)$ (on/off ratio: 2.0×10^2). Given the factor that the charge mobility of P3HT-based FET is influenced by parameters including crystallite size, crystallite orientation, and interface morphology, this observation suggests

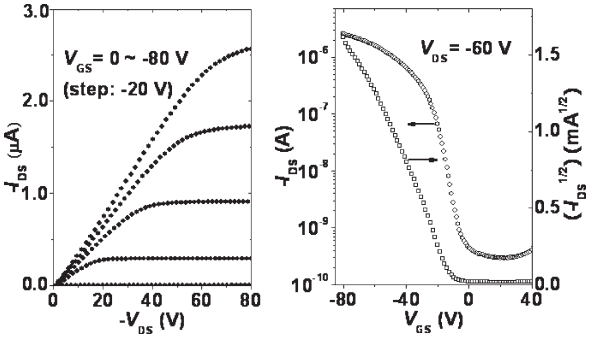

Figure 4. Electrical characteristics of FET fabricated by P3HT nanoribbon film. (A) Output characteristics (channel width: $W = 3$ μm; channel length: $L = 200$ μm) and (B) corresponding transfer and $-I_{DS}^{1/2} \sim V_{GS}$ curve.

that high ordered P3HT nanoribbon and its large crystalline size may be one of the factors that contribute to a good charge transport property. In addition, the charge transport property of the nanoribbon films shows a less dependence on surface treatment of the FET device owning to the preformed crystalline structures. More detailed work on charge mobility of 2D nanoribbons will be published elsewhere.

In contrast to P3HT with fully extended polymer chains, 1D nanowhisker aggregates (Figure S4) were the only structures observed from folded chain samples (samples C and D) with increased P3HT concentrations in anisole. The nanowhiskers aggregates cannot be separated by diluting the suspension, suggesting that P3HT chains partially incorporate in multiple nanowhiskers and generate intercrystalline links. Other marginal solvents (cyclohexanone and methyl benzoate) and mixed solvents (marginal solvents and DMF with different ratios) gave similar 1D nanowhisker aggregates when used to prepare ribbon-like P3HT crystals. These results suggest that the further growth of 1D nanowhisker via alkyl interactions is inhibited. We speculate that the P3HT chain folding leads to poorly defined surfaces of nanowhiskers similar to the defects in crystals, inhibiting the further growth of nanowhiskers (Figure S5). In contrast, intact surface of 1D nanowhiskers prepared from low molecular weight P3HT with extended polymer chains allows the further growth of nanowhiskers into nanoribbons.

With further increased concentration (> 1.5 mg/mL), both folded-chain and extended-chain P3HT samples form gels. The gels of folded-chain samples, similar to the observed nanowhisker aggregates, are composed of 1D nanowhiskers,[21] while the gels of extended-chain samples are composed of 2D nanoribbons (Figure S6). According to the P3HT crystalline structures investigated at high concentration, we believe that 1D nanowhiskers and 2D nanoribbons are fundamental structures in polycrystalline films prepared by folded-chain samples and extended-chain samples, respectively. Therefore, chain folding of P3HT plays an important role in determining crystalline structures of active films applied in organic electronics. Such behavior limits the P3HT crystal size by inhibiting the further growth of 1D nanowhiskers in polycrystalline films. It is believed that less alkyl side chain interaction and higher polymer backbone rigidity can inhibit the chain folding.[32,33] Therefore, conductive polymers with tailor-made crystalline dimension can be designed by tuning side chain interaction and polymer backbone rigidity.

In conclusion, we systematically investigated the P3HT crystallization in solutions by changing the molecular weight, crystallization temperature, and solution concentration. Molecular weight dependent chain folding and temperature determined fold length, which are typical crystallization behavior of flexible semicrystalline polymers, were observed when P3HT crystallized

in dilute solutions. P3HT polymer chain varies from extending to folding in crystals (1D nanowhiskers) when the M_n is above a critical value (10 kDa, determined by GPC). The fold length (nanowhisker width) can be controlled by crystallization temperature. 1D nanowhiskers with fully extended polymer chains can further grow into 2D nanoribbons with increased P3HT concentration while the further growth of nanowhiskers with folded chains is inhibited by the poorly defined surfaces. The nanoribbon aspect ratio is influenced by polymer molecular weight. The charge mobility of the 2D nanoribbon film was measured to be 0.012 $cm^2/(V\ s)$ with an on/off ratio of 6.5×10^4, which is higher than that of the P3HT films solution-cast from the same P3HT. The 1D nanowhiskers and 2D nanoribbons constitute the fundamental structures in polycrystalline P3HT films depending on the P3HT molecular weight. Traditional flexible semicrystalline polymer crystallization theory provides an easy avenue to understanding P3HT crystallization. Studying polymer crystallization in dilute solutions provides a simple way to understand the crystallization nature of conductive polymers and offer a physical control of their crystal dimensions.

Acknowledgment. This work is supported by National Science Foundation CAREER Award DMR 0746499. We thank Dr. Q. Zhang at Advanced Materials Processing and Analysis Center, University of Central Florida, for assistance of TEM characterization.

Supporting Information Available: Synthesis and the characterization of P3HT, preparation of P3HT crystals, and the fabrication of FET devices. This material is available free of charge via the Internet at http://pubs.acs.org.

References and Notes

(1) Thompson, B. C.; Fréchet, J. M. J. *Angew. Chem., Int. Ed.* **2008**, *47*, 58–77.
(2) Dennler, G.; Scharber, M. C.; Brabec, C. J. *Adv. Mater.* **2009**, *21*, 1–16.
(3) Zaumseil, J.; Sirringhaus, H. *Chem. Rev.* **2007**, *107*, 1296–1232.
(4) Yang, H.; Shin, T. J.; Yang, L.; Cho, K.; Ryu, C. Y.; Bao, Z. *Adv. Funct. Mater.* **2005**, *15*, 671–676.
(5) Jimison, L. H.; Toney, M. F.; McCulloch, I.; Heeney, M.; Salleo, A. *Adv. Mater.* **2009**, *21*, 1568–1572.
(6) Salleo, A. *Mater. Today* **2007**, *10*, 38–45.
(7) Bao, Z.; Dodabalapur, A.; Lovinger, A. J. *Appl. Phys. Lett.* **1996**, *69*, 4108.
(8) Li, G.; Shrotriya, V.; Yao, Y.; Yang, Y. *J. Appl. Phys.* **2005**, *98*, 043704.
(9) Lu, G.; Li, L.; Yang, X. *Adv. Mater.* **2007**, *19*, 3594–3598.
(10) Yang, H.; LeFevre, S. W.; Ryu, C. Y.; Bao, Z. *Appl. Phys. Lett.* **2007**, *90*, 172116.
(11) Joshi, S.; Grigorian, S.; Pietsch, U.; Pingel, P.; Zen, A.; Neher, D.; Scherf, U. *Macromolecules* **2008**, *41*, 6800–6808.
(12) Kline, R. J.; McGehee, M. D.; Kadnikova, E. N.; Liu, J.; Fréchet, J. M. J. *Adv. Mater.* **2003**, *15*, 1519–1522.
(13) Kline, R. J.; McGehee, M. D.; Toney, M. F. *Nat. Mater.* **2006**, *5*, 222–228.
(14) Zen, A.; Saphiannikova, M.; Neher, D.; Grenzer, J.; Grigorian, S.; Pietsch, U.; Asawapirom, U.; Janietz, S.; Scherf, U.; Lieberwirth, I.; Wegner, G. *Macromolecules* **2006**, *39*, 2162–2171.
(15) Yong, R. J. *Introduction to Polymers*; Chapman and Hall: London, 1981; pp 188−193.
(16) Briseno, A. L.; Mannsfeld, S. C. B.; Jenekhe, S. A.; Bao, Z.; Xia, Y. *Mater. Today* **2008**, *11*, 38–47.
(17) Samitsu, S.; Shimomura, T.; Heike, S.; Hashizume, T.; Ito, K. *Macromolecules* **2008**, *41*, 8000–8010.
(18) Berson, S.; Gettignies, R. D.; Bailly, S.; Guillerez, S. *Adv. Funct. Mater.* **2007**, *17*, 1377–1384.
(19) Xin, H.; Kim, F. S.; Jenekhe, S. A. *J. Am. Chem. Soc.* **2008**, *130*, 5424–5425.
(20) Liu, J.; Zou, J.; Zhai, L. *Macromol. Rapid Commun.* **2009**, *30*, 1387–1391.
(21) Ihn, K. J.; Moulton, J.; Smith, P. *J. Polym. Sci., Part B: Polym. Phys.* **1993**, *31*, 735–742.
(22) Yang, H.; Shin, T. J.; Bao, Z.; Ryu, C. Y. *J. Polym. Sci., Part B: Polym. Phys.* **2007**, *45*, 1303–1312.
(23) Chang, J.; Clark, J.; Zhao, N.; Sirringhaus, H.; Breiby, D. W.; Andreasen, J. W.; Nielsen, M. M.; Giles, M.; Heeney, M.; McCulloch, I. *Phys. Rev. B* **2006**, *74*, 115318.
(24) Zhang, R.; Li, B.; Iovu, M. C.; Jeffries-EL, M.; Sauv, G.; Copper, J.; Jia, S.; Tristram-Nagle, S.; Smilgies, D. M.; Lambeth, D. N.; McCullough, R. D.; Kowalewski, T. *J. Am. Chem. Soc.* **2006**, *128*, 3480–3481.
(25) The marginal solvent is a poor solvent for P3HT at room temperature and a good solvent for P3HT at elevated temperature. For samples B, C, and D, anisole was used as the marginal solvent. Sample A can dissolve in anisole at room temperature because of its low M_n. DMF was used as a cosolvent to decrease the solubility of anisole.
(26) Ungar, G.; Stejny, J.; Keller, A.; Bidd, I.; Whiting, M. C. *Science* **1985**, *229*, 386–389.
(27) Magonov, S. N.; Yerina, N. A. *Langmuir* **2003**, *19*, 500–504.
(28) Mena-Osteritz, E.; Meyer, A.; Langeveld-Voss, B. M. W.; Janssen, R. A. J.; Meijer, E. W.; Bäuerle, P. *Angew. Chem., Int. Ed.* **2000**, *39*, 2680–2684.
(29) Grévin, B.; Rannou, P.; Payerne, R.; Pron, A.; Travers, J. *Adv. Mater.* **2003**, *15*, 881–884.
(30) Schultz, J. M. *Polymer Crystallization: the Development of Crystalline Order in Thermoplastic Polymers*; American Chemical Society: Washington, DC, 2001; pp 53−56.
(31) Cho, S.; Lee, K.; Yuen, J.; Wang, G.; Moses, D.; Heeger, A. J.; Surin, M.; Lazzaroni, R. *J. Appl. Phys.* **2006**, *100*, 114503.
(32) Kline, R. J.; DeLongchamp, D. M.; Fischer, D. A.; Lin, E. K.; Richter, L. J.; Chabinyc, M. L.; Toney, M. F.; Heeney, M.; McCulloch, I. *Macromolecules* **2007**, *40*, 7960–7965.
(33) McCulloch, I.; Heeney, M.; Bailey, C.; Genevicius, K.; Macdonald, I.; Shkunov, M.; Sparrowe, D.; Tierney, S.; Wagner, R.; Zhang, W.; Chabinyc, M. L.; Kline, R. J.; McGehee, M. D.; Toney, M. F. *Nat. Mater.* **2006**, *5*, 328–333.